



Original article

Design, synthesis and antibacterial activity of fluoroquinolones containing bulky arenesulfonyl fragment: 2D-QSAR and docking study

Alaa A.-M. Abdel-Aziz^{a,b,*}, Yousif A. Asiri^c, Mohamed H.M. Al-Agamy^d^a Department of Pharmaceutical Chemistry, College of Pharmacy, King Saud University, Riyadh 11451, Saudi Arabia^b Department of Medicinal Chemistry, Faculty of Pharmacy, University of Mansoura, Mansoura 35516, Egypt^c Department of Clinical Pharmacy, College of Pharmacy, King Saud University, Riyadh 11451, Saudi Arabia^d Department of Pharmaceutics and Microbiology, College of Pharmacy, King Saud University, Riyadh 11451, Saudi Arabia

ARTICLE INFO

Article history:

Received 15 July 2011

Received in revised form

5 September 2011

Accepted 7 September 2011

Available online 16 September 2011

Keywords:

Fluoroquinolones
Arenesulfonamido
Antibacterial
2D-QSAR
Molecular docking

ABSTRACT

Here in, we report the design, synthesis, and antibacterial activity of series of bulky arenesulfonamido derivatives using ciprofloxacin and norfloxacin as scaffolds. All the synthesized compounds were investigated *in vitro* for their antibacterial activities against two Gram-positive and two Gram-negative organisms using dilution broth method. Among the tested compounds examined, compounds **3–7** showed significance difference from the standard drug ciprofloxacin. 2D-QSAR study provides details on the fine relationship linking structure and activity and offers clues for structural modifications that can improve the activity. Docking study of the compound **3b** into the active site of the topoisomerase II DNA-gyrase enzymes revealed a similar binding mode to ciprofloxacin with additional classical and nonclassical hydrogen bonds.

© 2011 Elsevier Masson SAS. All rights reserved.

1. Introduction

The fluoroquinolone antibacterial agents have been found to be one of the fastest growing groups of drugs in recent years [1–7]. They are compounds of intense interest because of their broad antibacterial spectrum against both Gram-positive and Gram-negative bacteria and their *in vivo* chemotherapeutic efficacy [8–10]. The fluoroquinolones are the only direct inhibitors of DNA synthesis by binding to the enzyme–DNA complex; they stabilize DNA strand breaks created by DNA gyrase and topoisomerase IV. Ternary complexes of drug, enzyme, and DNA block progress of the replication fork [7]. The inhibition of DNA gyrase and cell permeability of quinolones is greatly influenced by the nature of C-7 substituent on the standard structure of 4-quinolone-3-carboxylic acid [11,12]. During recent years a number of quinolones with substitution on piperazine ring at C-7 position of the basic structure of quinolones were synthesized and evaluated for antibacterial activities [13–16]. Most of these agents are substituted at the 7 position by a nitrogen heterocycle. Ciprofloxacin and norfloxacin

[17–20] characterized by having a piperazine moiety at C-7, which represented a site of significant modification. Recently, benzenesulfonamido fluoroquinolones (BSFQs) are a new class of fluoroquinolones (Fig. 1A and B) reported previously by Manzo et al. [21,22]. Some of those BSFQs have exhibited high *in vitro* activity against *Staphylococcus aureus* ATCC 29213 [23,24] and also against other Gram-positive clinical strains [25]. The new compounds would exert their biological action through a quinolone-like mechanism of action [23]. It was also reported that BSFQs have displayed a more favorable kinetics of access to the bacterial cell in *S. aureus* ATCC 29213 [23]. Studies on *Staphylococcus pneumoniae* and *S. aureus* have identified the BSFQs as “dual targeting” agents [26,27]. It was reported that the new analogs with a sulfa moiety on piperazinyl group inhibit *Escherichia coli* DNA gyrase in similar way as ciprofloxacin [23]. According to the proposed mechanisms of action of fluoroquinolones, substituent at 7-position of quinolone ring would be involved in the interaction with the enzyme through electrostatic forces [12,19,28].

In this context, the present work describes the synthesis, the investigation of the antibacterial properties of new bulky arenesulfonylquinolones (Fig. 1C–G) and the achievement of a better antibacterial profile at lower concentrations. The strategy is intended to obtain potent broad spectrum antibacterial activity using traditional medicinal chemistry techniques motivated by the comparative modeling of quinolones (A–G) together with the

* Corresponding author. Department of Pharmaceutical Chemistry, College of Pharmacy, King Saud University, Riyadh 11451, Saudi Arabia. Tel.: +966 56 2947305; fax: +966 1 4676220.

E-mail address: alaa_moenes@yahoo.com (A.A.-M. Abdel-Aziz).

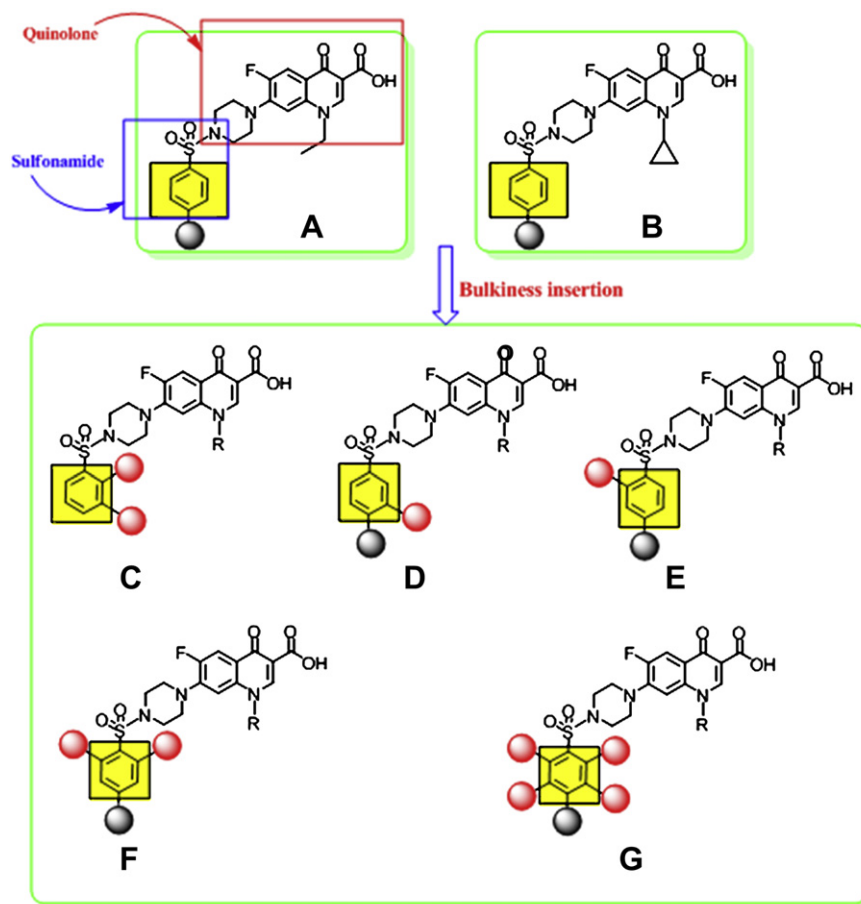


Fig. 1. Reported benzenesulfonamidonorfloxacin (A) and ciprofloxacin (B) and designed bulky arenesulfonyl derivatives (C–G).

available pharmacophore. Our strategy for synthesis such derivatives based on the modification of the structure of the known potent norfloxacin and ciprofloxacin. Moreover we describe a 2D-QSAR analysis for the complete series of arenesulfonylquinolones as well. Multiple linear regression analysis correlates biological activity values with various descriptors. Computer docking technique plays an important role in the drug design and discovery, as well as in the mechanistic study by placing a molecule into the binding site of the target macromolecule in a non-covalent fashion [29–33], and to predict the correct binding geometry for each ligand at the active site, which reveals the MOE score values and hydrogen bonds formed with the surrounding amino acids. MOE as flexible docking program enable us to predict favorable protein–ligand complex structures with reasonable accuracy and speed [34].

2. Results and discussion

2.1. Chemistry

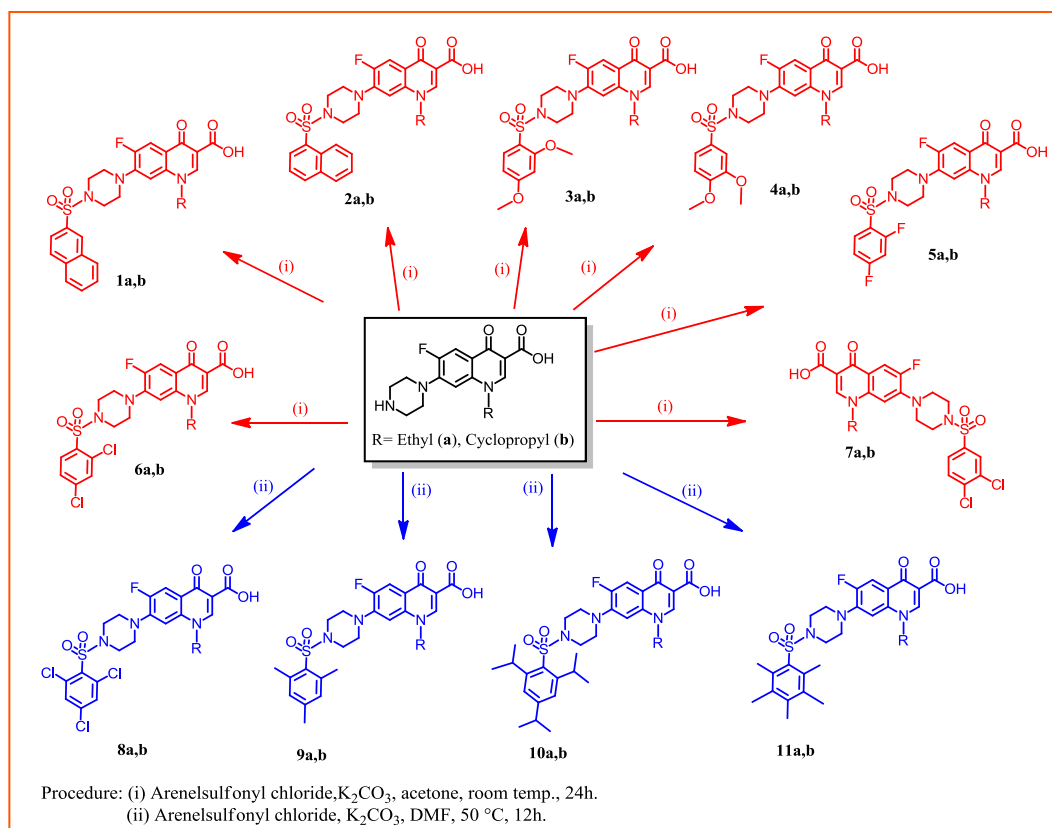
2.1.1. Synthesis of compounds 1–11

Scheme 1 outlines the synthetic pathway used to obtain compounds (1–11). Derivatives 1–7 were prepared by allowing norfloxacin (a) or ciprofloxacin (b) to react with the appropriate arenesulfonyl chloride in the presence of acetone and K_2CO_3 at room temperature for 24 h. On the other hand compounds 8–11 were obtained in relatively good yields by addition of the appropriate arenesulfonyl chloride to a stirred solution of norfloxacin (a) or ciprofloxacin (b) and K_2CO_3 in DMF at 50 °C for 12 h.

2.2. Biological activity

2.2.1. Antibacterial activities and structural–activity relationships

Compounds 1–11 in addition to the reference ciprofloxacin were tested for their *in vitro* antibacterial activity against two Gram-negative (*E. coli* ATCC 25922 and *Pseudomonas aeruginosa* ATCC 27853) and two Gram-positive (*S. aureus* ATCC 29213 and *Bacillus subtilis* ATCC 10400) microorganisms. The minimal inhibitory concentrations (MIC in $\mu\text{g/mL}$ and $\mu\text{mol/mL}$) or the lowest drug concentrations that prevent visible growth of bacteria (Table 1), were determined by a standard broth micro-dilution technique using the European Committee for Antimicrobial Susceptibility Testing (EUCAST) and Laboratory Standards method [35]. The results of MIC tests against Gram-positive and Gram-negative bacteria revealed that ciprofloxacin derivatives ($R = \text{cyclopropyl}$) were usually more active than norfloxacin derivatives ($R = \text{ethyl}$) especially against Gram-positive pathogens. From the obtained data (Table 1), the 3,4- and 2,4-disubstituted benzenesulfonyl derivatives 3–4 and 6–7 exhibited potential activity against all the tested Gram-positive organism (MIC; 0.000463–0.000481 $\mu\text{mol/mL}$), which was more pronounced than that exhibited by the reference, ciprofloxacin (MIC; 0.000758 $\mu\text{mol/mL}$). The 1-naphthalenesulfonyl derivative 2b (MIC; 0.000479 $\mu\text{mol/mL}$) revealed a better activity two times more active than ciprofloxacin (MIC; 0.000758 $\mu\text{mol/mL}$) against *B. subtilis* while the inhibition was moderate to weak with other tested strains. Similarly compounds 5b (MIC; 0.000493 $\mu\text{mol/mL}$), 8a (MIC; 0.000444 $\mu\text{mol/mL}$) and 8b (MIC; 0.000435 $\mu\text{mol/mL}$), showed selective activity against *B. subtilis* two times more active than ciprofloxacin with lower activity against other strain. Other



Scheme 1. Synthesis of bulky arenesulfonylquinolones.

compounds showed variable inhibition activities against the used strains. Moreover, *in vitro* assay results revealed that the antibacterial potency of target quinolone **9–11** was mild for Gram-positive and Gram-negative strains (MIC; 0.00798 to ≥ 0.473 $\mu\text{mol/mL}$). These results indicated that the aliphatic substitution did not play an

important role in the antibacterial potency as the activity decreased when the number of alkyl group or steric bulkiness increased from compounds **9** to compounds **11** which were the least active derivatives. However, the antibacterial potencies of the disubstituted arenesulfonylquinolones **3–7** were all superior to that of trisubstituted

Table 1
Minimum inhibitory concentrations of the designed arenesulfonylquinolones.

Compd. no.	<i>S. aureus</i> ATCC 29213		<i>B. subtilis</i> ATCC 10400		<i>E. coli</i> ATCC 25922		<i>P. aeruginosa</i> ATCC 27853	
	MIC ($\mu\text{g/mL}$)	MIC ($\mu\text{mol/mL}$)	MIC ($\mu\text{g/mL}$)	MIC ($\mu\text{mol/mL}$)	MIC ($\mu\text{g/mL}$)	MIC ($\mu\text{mol/mL}$)	MIC ($\mu\text{g/mL}$)	MIC ($\mu\text{mol/mL}$)
1a	1	0.00196	0.5	0.000981	128	0.251	64	0.126
1b	1	0.00192	1	0.00192	64	0.123	128	0.245
2a	1	0.00196	0.5	0.000981	128	0.251	128	0.251
2b	1	0.00192	0.25	0.000479	32	0.0613	64	0.123
3a	0.25	0.000481	0.25	0.000481	≤ 0.25	≤ 0.000481	2	0.00385
3b	≤ 0.25	≤ 0.000470	≤ 0.25	≤ 0.000470	≤ 0.25	≤ 0.000470	0.25	0.000470
4a	0.5	0.000962	0.5	0.000962	≤ 0.25	≤ 0.000481	2	0.00385
4b	≤ 0.25	≤ 0.000470	0.25	0.000470	≤ 0.25	≤ 0.000470	2	0.00376
5a	4	0.00807	2	0.00404	4	0.00807	64	0.129
5b	2	0.00394	0.25	0.000493	4	0.00788	32	0.063
6a	0.25	≤ 0.000473	0.25	0.000473	≤ 0.25	≤ 0.000473	1	0.00139
6b	≤ 0.25	≤ 0.000463	≤ 0.25	≤ 0.000463	≤ 0.25	≤ 0.000463	1	0.00185
7a	≤ 0.25	≤ 0.000473	≤ 0.25	≤ 0.000473	≤ 0.25	≤ 0.000473	1	0.00189
7b	≤ 0.25	≤ 0.000463	≤ 0.25	≤ 0.000463	≤ 0.25	≤ 0.000463	1	0.00185
8a	1	0.001776	0.25	0.000444	≥ 256	≥ 0.455	≥ 256	≥ 0.455
8b	1	0.00174	0.25	0.000435	64	0.111	64	0.111
9a	4	0.00798	4	0.00798	16	0.032	32	0.064
9b	32	0.062	16	0.031	32	0.062	64	0.125
10a	32	0.055	32	0.055	32	0.055	64	0.109
10b	128	0.214	64	0.107	2	0.00335	≥ 256	≥ 0.428
11a	128	0.242	128	0.242	128	0.242	128	0.242
11b	≥ 256	≥ 0.473	128	0.236	≥ 256	≥ 0.473	≥ 256	≥ 0.473
Ciprof.	≤ 0.25	≤ 0.000758	≤ 0.25	≤ 0.000758	≤ 0.25	≤ 0.000758	0.25	0.000758

arenesulfonylquinolones **8–11** such as compounds **6–7** are broad spectrum antibacterial compared with compounds **8** which are selective only for *B. subtilis*. The activities of quinolones **3–4** and **6–7** were comparable to quinolones **5**, and the results indicated that the fluoro group at the 2,4-position of the arenesulfonyl fragment did not play an essential role in influencing the potency except for its selectivity to *B. subtilis* in which **5b** (MIC; 0.000493 $\mu\text{mol/mL}$) is two times active than ciprofloxacin regarding this strain. More interestingly, the 2,4-dimethoxybenzenesulfonylquinolone **3b** exhibited excellent activities against all the strains. It provided the most effective antibacterial activity against *S. aureus* ATCC 29213 (MIC; ≤ 0.000470 $\mu\text{mol/mL}$), *B. subtilis* ATCC 10400 (MIC; ≤ 0.000470 $\mu\text{mol/mL}$), *E. coli* ATCC 25922 (MIC; ≤ 0.000470 $\mu\text{mol/mL}$) and *P. aeruginosa* ATCC 27853 (MIC; 0.000470 $\mu\text{mol/mL}$) and was more potent than the reference drug ciprofloxacin (MIC; ≤ 0.000758 $\mu\text{mol/mL}$).

2.3. Molecular modeling results

2.3.1. 2D-QSAR study

The antibacterial activities of the tested compounds, presented in $-\log 1/\text{MIC}$ (Table 2), were used in the 2D-QSAR studies using VLife Molecular Design Suite [36]. Compounds were divided into training and test set. This was achieved by setting aside five compounds as test set which have regularly distributed activity. Selection of molecules in the training set and test is a key and important feature of any QSAR model. Therefore the care was taken in such a way that biological activities of all compounds in test set lie within the maximum and minimum value range of biological activities of training set of compounds. A Uni-Column statistics for training set and test set were generated to check correctness of selection criteria for trainings and test set molecules. The maximum and minimum value in training and set were compared in a way that:

1. The maximum value of $-\log 1/\text{MIC}$ of test set should be less than or equal to maximum value of $-\log 1/\text{MIC}$ of training set.
2. The minimum value of $-\log 1/\text{MIC}$ of test set should be higher than or equal to minimum value of $-\log 1/\text{MIC}$ of training set.

This observation showed that test set was interpolative and derived within the minimum–maximum range of training set. The mean and standard deviation of $-\log 1/\text{MIC}$ values of sets of training and test provide insights to relative difference of mean and point density distribution of two sets. 2D-QSAR models were generated for training set of 18 compounds using multiple linear regression (MLR) method. The best QSAR model was selected on the basis of value of statistical parameters like r^2 (square of correlation coefficient for training set of compounds), q^2 (cross-validated r^2), and pred_r^2 (predictive r^2 for the test set of compounds). All QSAR model was validated and tested for its predictability using an external test set of five compounds. Statistical results generated by 2D-QSAR analysis showed that QSAR models have good internal as well as external predictability (Table 3). The results obtained for actual and predicted activity are presented in Table 2 and the residuals were found to be minimal. The regression equation obtained for the different series of compounds is given below.

- 2D-QSAR model for antibacterial activity against *S. aureus* (Model 1)

$$-\log 1/\text{MIC} = -0.2078(\pm 0.0085) \text{SsCH3E-index} + 0.0971(\pm 0.0136) \text{SssOE-index} - 0.3033(\pm 0.0974) \text{T_C_F_7} + 0.1830(\pm 0.0777) \text{T_2_Cl_5} + 3.4353$$

- 2D-QSAR model for antibacterial activity against *B. subtilis* (Model 2)

$$-\log 1/\text{MIC} = -0.2098(\pm 0.0192) \text{SsCH3E-index} + 0.0815(\pm 0.0201) \text{SssOE-index} + 3.2329$$

- 2D-QSAR model for antibacterial activity against *E. coli* (Model 3)

$$-\log 1/\text{MIC} \text{E. coli} = -0.4727(\pm 0.0010) \text{T_C_C_1} - 0.9587(\pm 0.0127) \text{T_Cl_Cl_4} + 1.9205(\pm 0.0326) \text{k3alpha} + 13.8546(\pm 1.6427) \text{SdsCHE-index} + 0.1435(\pm 0.0023) \text{SaaCHcount} - 14.8499$$

Table 2

Observed and predicted antibacterial activity ($-\log 1/\text{MIC}$) of the designed arenesulfonylquinolones.

Compd. no.	<i>S. aureus</i>		<i>B. Subtilis</i>		<i>E. coli</i>		<i>P. aeruginosa</i>	
	Observed	Predicted	Observed	Predicted	Observed	Predicted	Observed	Predicted
1a	2.71	2.76	3.01	2.85	0.60	0.68	0.90	0.99
1b	2.72	2.83	2.72	3.23	0.91	1.05	0.61	1.16
2a	2.71	2.76	3.01	2.85	0.60	0.87	0.60	0.41
2b	2.72	2.83	3.32	3.10	1.21	0.87	0.91	0.58
3a	3.32	3.17	3.32	3.10	3.32	3.38	2.14	1.85
3b	3.33	3.24	3.33	3.48	3.33	3.52	3.33	2.03
4a	3.02	3.17	3.02	3.10	3.32	3.39	2.14	2.30
4b	3.33	3.24	3.33	3.47	3.33	3.53	2.42	2.48
5a	2.09	2.16	2.39	2.87	2.09	1.86	0.89	1.15
5b	2.41	2.22	3.31	3.23	2.10	2.01	1.20	1.32
6a	3.33	2.94	3.33	2.85	3.33	2.45	2.86	1.57
6b	3.33	3.01	3.33	3.23	3.33	3.40	2.73	1.74
7a	3.33	3.30	3.33	2.85	3.33	2.32	2.72	2.77
7b	3.33	3.38	3.33	3.23	3.33	3.26	2.73	2.94
8a	2.75	2.94	3.35	2.85	0.34	0.71	0.34	0.98
8b	2.76	3.01	3.36	3.23	0.95	0.87	0.95	1.15
9a	2.09	1.59	2.09	1.68	1.49	1.46	1.19	0.55
9b	1.21	1.66	1.51	2.06	1.21	1.63	0.90	0.72
10a	1.26	Outlier	1.26	Outlier	1.26	1.32	0.96	Outlier
10b	0.67	0.25	0.97	0.63	2.47	1.45	0.37	0.22
11a	0.62	0.74	0.62	0.82	0.62	0.27	0.62	0.39
11b	0.33	0.81	0.63	1.20	0.33	0.46	0.33	0.56
Ciprof.	3.12	2.83	3.12	3.23	3.12	3.28	3.12	3.10

Table 3

Statistical results of 2D-QSAR models for arenesulfonylquinolones obtained by multiple linear regression method.

Entry	Statistical parameters	<i>S. aureus</i> (Model 1)	<i>B. Subtilis</i> (Model 2)	<i>E. Coli</i> (Model 3)	<i>P. Aureognosa</i> (Model 4)
1	r^2	0.9268	0.9026	0.9404	0.7940
2	q^2	0.8695	0.8569	0.8727	0.6728
3	Pred_ r^2	0.6734	0.6160	0.5677	0.5259
4	r^2_{se}	0.2853	0.2973	0.3512	0.4225
5	q^2_{se}	0.3550	0.3737	0.4133	0.5586
6	Pred_ r^2_{se}	0.3674	0.2915	0.5355	0.6164
7	Best-Ran Q^2	0.14369	0.21319	0.48605	0.29079
8	Z-score Q^2	2.05333	7.83318	6.40195	2.86240
9	F-test	41.1690	64.8589	41.0142	17.9911

- 2D-QSAR model for antibacterial activity against *P. aeruginosa* (Model 4)

$$-\log 1/\text{MIC} = -0.3388 \text{ T_T_N_4} + 0.1364 \text{ SssOE-index} + 0.3572 \text{ T_2_Cl_5} - 0.4756 \text{ T_C_S_5} + 5.8340$$

The statistical result of 2D-QSAR models is tabulated in Table 3. A brief idea of the requirement of different physicochemical parameters and their contributions (positive or negative influence on biological activity), required for potential antibacterial activity was obtained. The regression equation so obtained will be useful for the prediction of biological activities of the designed series of compounds, in future.

2.3.1.1. Contribution of descriptors

2.3.1.1.1. For Gram-positive bacteria. The statistical best models (Model 1) for antibacterial activity against *S. aureus* with a coefficient of determination (r^2) = 0.9268 was considered, as the model showed an internal predictive power (q^2 = 0.8695) of 86% and a predictivity for the external test set (pred_ r^2 = 0.6734) of about 67%. Moreover the statistical best model for antibacterial activity against *B. subtilis* (Model 2) showed similar pattern with a coefficient of determination (r^2) = 0.9026 was considered, as the model showed an internal predictive power (q^2 = 0.8569) of 86% and a predictivity for the external test set (pred_ r^2 = 0.6160) of about 62%. The descriptor SsCH3E-index is electrotopological state indices for number of $-\text{CH}_3$ group connected with one single bond. This descriptor showed negative contribution toward Gram-positive *S. aureus* and *B. subtilis* in selected models (Model 1 and Model 2) and its contributions are approx 54% and 73% respectively. Negative contribution of this descriptor revealed the decrease of anti-Gram-positive bacteria of arenesulfonylquinolones with the presence of CH_3 group such as compounds **10a** and **10b**. On the other hand descriptor such as SssOE-index which is electrotopological state indices for number of oxygen atom connected with two single bonds showed positive contribution toward both strain of Gram-positive with contribution of 20% and 27% for *S. aureus* and *B. subtilis*, respectively. Such positive effect indicated that the antibacterial activity was increased with the presence of methoxy groups such as compounds **3** and **4**. Moreover Model 1 for *S. aureus* showed two additional descriptors, one is T_C_F_7 which is the count of number of carbon atom (single, double or triple bonded) separated from fluorine by seven bonds and the second is T_2_Cl_5 which is the count of number of double bonded atoms (i.e. any double bonded atom, T_2) separated from chlorine atom by five bonds in a molecule. The first descriptor showed negative contribution and its value was 15% which revealed the decrease in anti-*S. aureus* activity with the presence of fluorine atoms on arenesulfonyl fragment as indicated with compounds **5a**. On contrary the second descriptor is positively contributed with

anti-*S. aureus* activity (11%) which revealed the increased activity with the presence of chlorine atoms on arenesulfonyl moiety such as compounds **6** and **7**.

2.3.1.1.2. For Gram-negative bacteria. The statistical best models (Model 3) for antibacterial activity against *E. coli* with a coefficient of determination (r^2) = 0.9404 was considered, as the model showed an internal predictive power (q^2 = 0.8727) of 87% and a predictivity for the external test set (pred_ r^2 = 0.5677) of about 57%. Alignment Independent (AI) descriptors T_C_C_1 which mean the count of number of carbon atoms (single double or triple bonded) separated from carbon atom by 1 bond distances in a molecule and T_Cl_Cl_4 which mean the count of number of chlorine atoms (single double or triple bonded) separated from chlorine atom by 4 bond distances in a molecule. These two descriptors showed negative contribution toward antibacterial activity against *E. coli* in selected QSAR model-3 and the contributions are approx 35% and 20% respectively. Negative contributions of these descriptors revealed the decrease of antibacterial activity against *E. coli* of arenesulfonylquinolones with the presence of methyl and chlorine groups such as compounds **8–11**. K3alpha is a descriptor signifies third alpha modified shape index and is positively contributing descriptor toward anti-*E. coli* activity and its contribution is approx 22%. While SdsCHE-index is Electrotopological state indices for number of $-\text{CH}$ group connected with one double and one single bond in a molecule. This is the positively contributing toward antibacterial activity against *E. coli* and it contributes approx 16%. Lastly SaaCHcount is a descriptor defines the total number of carbon atoms connected with hydrogen along with two aromatic bonds and is 7% positively contributing descriptor toward anti-*E. coli* activity. Positive contributions of these descriptors were clearly signifying that the presence of quinolone pharmacophore was important for biological activity.

The statistical best models (Model 4) for antibacterial activity against *P. aeruginosa* with a coefficient of determination (r^2) = 0.7940 was considered, as the model showed an internal predictive power (q^2 = 0.6728) of 67% and a predictivity for the external test set (pred_ r^2 = 0.5259) of about 53%. Alignment Independent (AI) descriptors T_T_N_4 which mean the count of number of double bonds separated from nitrogen atom by four bond distances in a molecule and T_C_S_5 which mean the count of number of carbon atoms (single double or triple bonded) separated from sulphur atom by five bond distances in a molecule. These two descriptors showed negative contributions toward antibacterial activity against *P. aeruginosa* in selected QSAR Model 4 and the contributions are approx 27% and 21% respectively. Negative contributions of these descriptors revealed the decrease of antibacterial activity against *P. aeruginosa* of arenesulfonylquinolones with the presence of methyl group such as compounds **9–11**. Moreover descriptors, such as SssOE-index which are electrotopological state indices for number of oxygen atom connected with two single bonds and Alignment Independent (AI) descriptors T_2_Cl_5 which mean the count of number of double bond separated from chlorine atom by five bond distances in a molecule, showed positive contribution toward *P. aeruginosa* with contributions of 35% and 17% respectively. Such positive effect indicates that the antibacterial activity was increase with the presence of methoxy and chlorine moieties such as compounds **3** and **6**.

2.3.2. Field alignment

FieldAlign [37] was used to align the synthesized ligands to the most active arenesulfonylquinolone **3b**. The idea behind this type of alignment is that two molecules which bind to a common active site tend to make similar interactions with the protein and hence have highly similar field properties. Field alignment was used; taking into consideration the excluded volume provided by the binding site amino acid residues, to align the ligands to the most

active arenesulfonylquinolone **3b**, Fig. 2. The main constraints which have been used were the field points representing the hydrophobic moiety, the hydrogen bond donor and that representing the hydrogen bond acceptor. The compounds which are top ranked in similarity index turned to have potent antibacterial activity (Table 4). Investigating the alignment of these compounds show high degree of compliance with the essential features which were constrained (hydrogen bond donor and hydrogen bond acceptor and hydrophobic aromatic feature). Investigating the compounds which are the least active reveal a high score of excluded volume clash penalty (compounds **9–11**) or in general they show no perfect mapping with the constrained field points.

2.3.3. Docking studies

To predict the antimicrobial data on a structural basis, automated docking studies were carried out using MOE 2008.10 program [34] installed on 2.OG Core 2 Duo. The scoring functions and hydrogen bonds formed with the surrounding amino acids are used to predict the binding modes, the binding affinities and orientation of the docked compounds at the active site of the topoisomerase II DNA-gyrase enzymes. The protein–ligand complex was constructed based on the X-ray structure of topoisomerase II DNA-gyrase with its bound inhibitor ciprofloxacin that available through the RCSB Protein Data Bank (PDB entry 2XCT) [38]. The active site of the enzyme was defined to include residues within a 10.0 Å radius to any of the inhibitor atoms. The scoring functions of the compounds were calculated from minimized ligand protein complexes. In order to compare the binding affinity of the newly synthesized arenesulfonyl analogs, we docked compounds **3b** and **10b** with different activity into the empty binding site of topoisomerase II DNA gyrase (2XCT), with its bound inhibitor ciprofloxacin. Fig. 3 showed the docking solutions with the highest predicted binding affinity for topoisomerase II DNA gyrase, binding mode of the original ligand into its binding site and binding modes of compounds **3b** and **10b** as well. As a results of molecular docking and as shown from Fig. 3, the following results can be drawn: ciprofloxacin (the original ligand) reveals docking score of -16.50 kcal/mol and forms two hydrogen bonds with Arg-458 (2.81 Å) and Ser-1084 (2.79 Å) and another two co-ordinate bonds with Mn^{++} (Fig. 3; upper right panel). Compound **10b** which is the least active exhibits relatively weak binding affinity with docking score of -5.11 kcal/mol but similarly forms one hydrogen bond with Ser-1084 (2.79 Å), and another bond with Gly-459 (3.31 Å) (Fig. 3; lower right panel). The weak binding affinity of such compound **10b** may be attributed to steric clash of tri-isopropyl moieties with the adjacent residue and base pair. Compound **3b** which is the most active compound as antibacterial agent possess docking scores of -25.35 kcal/mol and forms three classical hydrogen bonds [31]

with Ser-1084 (2.80 Å), Gly-459 (2.84 Å, 2.56 Å) in addition to five nonclassical hydrogen bonds [31] with DC-13 (2.55 Å, 2.57 Å), Glu-477 (3.38 Å), Asn-475 (2.61 Å) and DC-14 (2.64 Å) (Fig. 3; lower left panel). Moreover both compounds **3b** and **10b** showed coordination bonds with Mn^{++} similar to ciprofloxacin. In short, compound **3b** can be bind in the active site of enzyme in approximately similar fashion of ciprofloxacin with an additional classical and nonclassical hydrogen bonds as described above, confirming the molecular design of the reported class of arenesulfonyl derivatives [21,22,39,40].

3. Conclusion

In the present investigation, 22 different bulky arenesulfonylquinolones based ciprofloxacin and norfloxacin scaffold were synthesized and evaluated for their antibacterial activity. Most compounds exhibited significant antibacterial activity. A remarkable activity was found in compounds **3** and **4** that carrying methoxy moieties. Compounds **6** and **7** with chloro substitution also exhibited excellent antibacterial activity. Amongst the compounds tested, **3b** and **6b** were found to be most potent, while **1**, **2**, and **8** were found to have an average activity. On the other hand series **9–11** was found to be the least active as antibacterial agents in this study. From the detailed analysis of the results of above studies, we conclude that antibacterial activity of the synthesized compounds significantly depends on the electronic effect of methoxy and chloro groups and this activity diminishes by methyl substitution which may attributed to steric reason. Various physicochemical indices are helpful for the understanding of microbiological results, as shown by our 2D-QSAR study. The 2D-QSAR results could not be addressed to a concrete drug–receptor interaction, but they can reveal trends in the relationship between ligand structures and their activities for our set of antibacterial agents. Analysis of 2D-QSAR models provides details on the fine relationship linking structure and activity and offers clues for structural modifications that can improve the activity. These trends should prove to be an essential guide for the future work. Molecular docking studies further supported the potent antibacterial inhibitory activity of **3b** compared to **10b** and ciprofloxacin and further help understanding the various interactions between the ligands and enzyme active sites in detail and thereby help to design novel potent quinolone derivatives.

4. Experimental

4.1. Chemistry

Melting points (uncorrected) were recorded on Barnstead Electrothermal 9100 melting apparatus. IR spectra were recorded

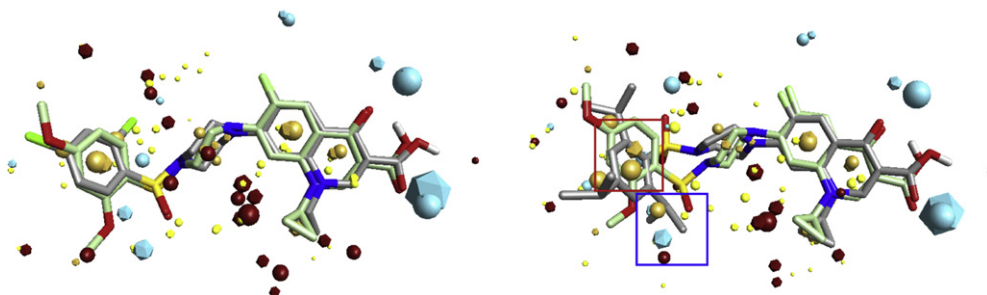


Fig. 2. Left panel showed that the most active arenesulfonylquinolones **3b** and **6b** were aligned together. Three constraints were applied. The first is the hydrophobic field point in the center of the arenesulfonyl fragment (yellow sphere), the second is the negative field point which represents H-bond donor on the protein (blue sphere) and the third is the positive field point which represents H-bond acceptor on the protein (red sphere). The field points interpretation is: blue, negative field points; red, positive field points; yellow, van der Waals surface field points; gold/orange, hydrophobic field points (describe regions with high polarisability/hydrophobicity). Right panel showed that the least active arenesulfonylquinolone **10b** aligned on the most active **3b** with steric and hydrophobic clash with applied field and lead to the noncompliance with the negative constrain and the hydrophobic constrain (for interpretation of the references to colour in this figure legend, the reader is referred to the web version of this article).

Table 4

Fieldalign similarity score of the newly synthesized ligands to that of the most active antibacterial arenesulfonylquinolone **3b**.^a

Compound no.	Similarity score	Compound No.	Similarity score
3a	0.757	5a	0.708
6b	0.755	5b	0.707
7b	0.752	2a	0.685
6a	0.749	1b	0.684
4b	0.742	11b	0.684
8b	0.742	1a	0.683
8a	0.739	11a	0.679
7a	0.736	9b	0.671
7a	0.733	9a	0.667
4a	0.729	10b	0.651
2b	0.708	10a	0.644

^a The top ranked ligands turned to have broad spectrum antibacterial. In general, scores are high and we focus on three major essential features in quinolones and neglect others.

on a FT-IR Perkin–Elmer spectrometer. ¹H NMR and ¹³C NMR were recorded in DMSO-d₆ and/or CDCl₃ on a Bruker 500 MHz instrument using TMS as internal standard (chemical shifts in δ ppm). Microanalytical data (C, H, and N) were performed on Perkin–Elmer 240 B analyzer and they agreed with proposed structures within $\pm 0.4\%$ of the calculated values. Mass spectra were recorded on a Perkin–Elmer, Clarus 600 GC/MS and Varian, TQ 320 GC/MS/MS mass spectrometers. Solvent evaporation was performed under reduced pressure using Buchan Rotatory Evaporator unless otherwise stated. Thin layer chromatography was performed

on precoated (0.25 mm) silica gel GF254 plates (E. Merck, Germany), compounds were detected with 254 nm UV lamp. Silica gel (60–230 mesh) was employed for routine column chromatography separations. Compounds **1b** and **9b** were prepared following their procedures reported in the literature [40].

4.1.1. General procedure for the synthesis of compounds **1–7**

A mixture of norfloxacin (**a**) or ciprofloxacin (**b**) (1 mmol) (Scheme 1) and K₂CO₃ (152 mg, 1.1 mmol) was stirred in acetone (20 mL) at room temperature for 20 min. To the resulted mixture, the appropriate arenesulfonyl chloride (1.2 mmol) in acetone (5 mL) was added dropwise over a period of 20 min. The reaction mixture was further stirred at room temperature for 24 h. The separated solid was then filtered, washed with cold water, dried and crystallized from the appropriate solvent.

4.1.1.1. 1-Ethyl-6-fluoro-7-(4-(naphthalen-2-ylsulfonyl)piperazin-1-yl)-4-oxo-1,4-dihydroquinoline-3-carboxylic acid (1a**)**. Yield, 88%; mp 290–291 °C (MeOH); IR(KBr) $\nu_{\text{max}}/\text{cm}^{-1}$ 3446 (OH), 1718 (C=O), 1640 (C=O). ¹H NMR (DMSO-d₆): δ 15.24 (s, br, 1H), 8.92 (s, 1H), 8.51 (s, 1H), 8.24–8.19 (m, 2H), 8.10–8.08 (d, 1H, $J = 7.5$ Hz), 7.86–7.80 (m, 2H), 7.75–7.71 (m, 2H), 7.17–7.16 (d, 1H, $J = 7.0$ Hz), 4.55–4.54 (d, 2H, $J = 6.0$ Hz), 3.41 (s, 4H), 3.19 (s, 4H), 1.36–1.33 (t, 3H, $J = 7.0$ Hz). ¹³C NMR: δ 176.08, 165.97, 153.69, 151.70, 148.54, 144.71, 144.63, 136.95, 134.52, 132.05, 131.80, 129.47, 129.37, 128.89, 127.72, 122.80, 119.69, 111.26, 111.08, 107.08, 106.57, 79.13, 49.01, 48.83, 45.65, 14.27 MS m/z (%); 509.60 (8.0, M⁺).

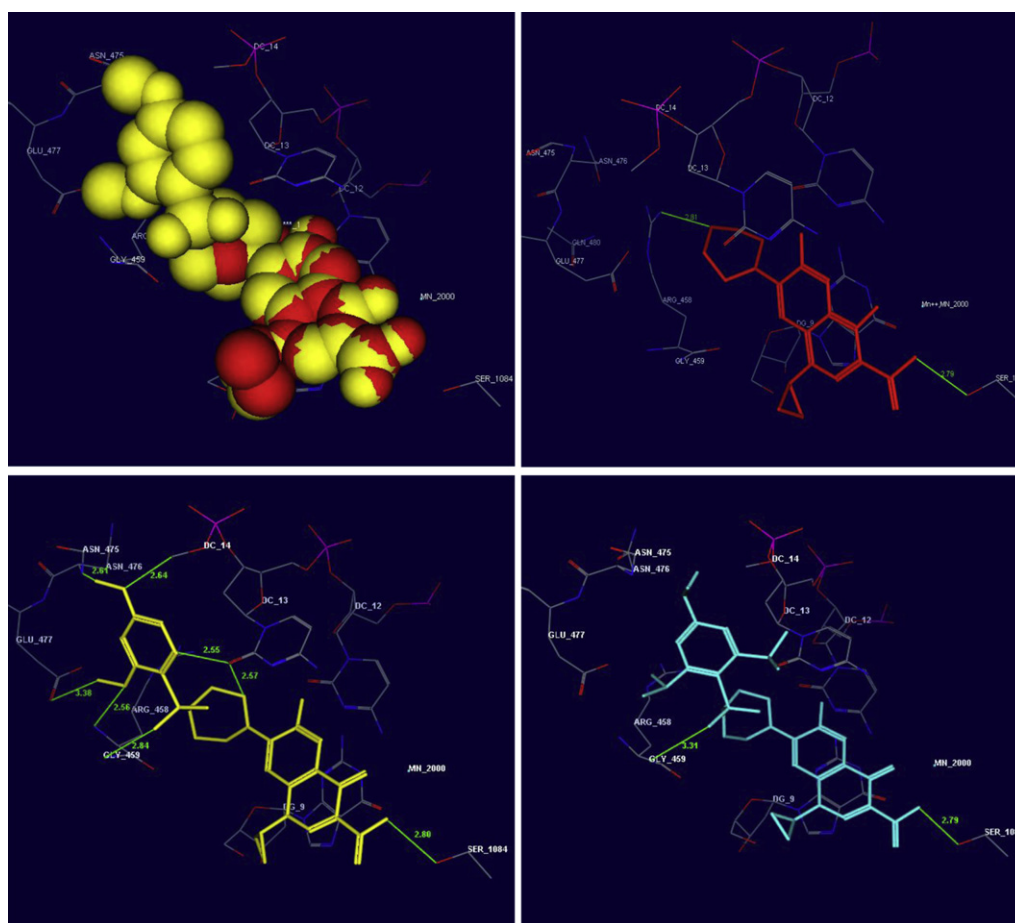


Fig. 3. The orientation of **3b** (color yellow) in DNA-gyrase active pocket (upper left panel; ciprofloxacin is shown as red). The docked ciprofloxacin (upper right panel; color red), **3b** (lower left panel; color yellow) and **10b** (lower right panel; color cyan) in DNA-gyrase active pocket (H bonds are shown as green) (for interpretation of the references to colour in this figure legend, the reader is referred to the web version of this article.)

4.1.1.2. 1-Cyclopropyl-6-fluoro-7-(4-(naphthalen-2-ylsulfonyl)piperazin-1-yl)-4-oxo-1,4-dihydroquinoline-3-carboxylic acid (1b). Yield, 85%; IR(KBr) $\nu_{\max}/\text{cm}^{-1}$ 3448 (OH), 1720 (C=O), 1633 (C=O). ^1H NMR (DMSO- d_6); δ 15.08 (s, br, 1H), 8.61 (s, 1H), 8.51 (s, 1H), 8.24–8.19 (m, 2H), 8.10–8.08 (d, 1H, $J = 7.5$ Hz), 7.82–7.79 (m, 2H), 7.76–7.69 (m, 2H), 7.53–7.51 (d, 1H, $J = 7.0$ Hz), 3.76 (s, 1H), 3.41 (s, 4H), 3.20 (s, 4H), 1.30–1.29 (d, 2H, $J = 5.5$ Hz), 1.11 (s, 2H). ^{13}C NMR; δ 176.24, 165.77, 153.79, 151.80, 147.96, 144.37, 144.29, 138.91, 134.52, 132.07, 131.80, 129.48, 129.36, 128.90, 127.87, 127.72, 122.80, 119.01, 111.00, 110.82, 106.95, 106.78, 79.14, 48.74, 45.61, 35.79, 7.50. MS m/z (%); 521.90 (4.0, M^+).

4.1.1.3. 1-Ethyl-6-fluoro-7-(4-(naphthalen-1-ylsulfonyl)piperazin-1-yl)-4-oxo-1,4-dihydroquinoline-3-carboxylic acid (2a). Yield, 90%; mp 218–219 °C (MeOH); IR(KBr) $\nu_{\max}/\text{cm}^{-1}$ 3446 (OH), 1735 (C=O), 1631 (C=O). ^1H NMR (DMSO- d_6); δ 15.24 (s, br, 1H), 8.90 (s, 1H), 8.71–8.69 (d, 1H, $J = 8.5$ Hz), 8.32–8.31 (t, 1H, $J = 8.0$ Hz), 8.22–8.21 (d, 1H, $J = 6.5$ Hz), 8.13–8.11 (d, 1H, $J = 8.0$ Hz), 7.83–7.67 (m, 4H), 7.14–7.12 (d, 1H, $J = 7.0$ Hz), 4.53–4.52 (d, 2H, $J = 6.5$ Hz), 3.40 (s, 4H), 3.32 (s, 4H), 1.35–1.33 (t, 3H, $J = 6.5$ Hz). ^{13}C NMR; δ 176.04, 165.96, 153.68, 151.69, 148.47, 144.64, 136.92, 134.80, 133.98, 131.80, 130.34, 129.35, 128.89, 128.32, 127.02, 124.52, 119.71, 119.65, 111.21, 111.03, 107.07, 106.53, 79.13, 48.99, 45.65, 14.30. MS m/z (%); 509.20 (5.0, M^+). Anal. calcd. For $\text{C}_{26}\text{H}_{24}\text{FN}_3\text{O}_5\text{S}$: C, 61.29; H, 4.75; N, 8.25; S, 6.29. Found: C, 61.32; H, 5.00; N, 8.44; S, 6.25.

4.1.1.4. 1-Cyclopropyl-6-fluoro-7-(4-(naphthalen-1-ylsulfonyl)piperazin-1-yl)-4-oxo-1,4-dihydroquinoline-3-carboxylic acid (2b). Yield, 87%; mp 249–250 °C (MeOH); IR(KBr) $\nu_{\max}/\text{cm}^{-1}$ 3446 (OH), 1723 (C=O), 1628 (C=O). ^1H NMR (DMSO- d_6); δ 15.11 (s, br, 1H), 8.72–8.70 (d, 1H, $J = 8.5$ Hz), 8.63 (s, 1H), 8.34–7.32 (d, 1H, $J = 8.5$ Hz), 8.23–8.21 (d, 1H, $J = 6.5$ Hz), 8.15–8.13 (d, 1H, $J = 8.0$ Hz), 7.86–7.84 (d, 1H, $J = 13.0$ Hz), 7.77–7.70 (m, 3H), 7.53–7.51 (d, 1H, $J = 7.5$ Hz), 3.76 (s, 1H), 3.36 (s, 8H), 1.28–1.27 (d, 2H, $J = 5.5$ Hz), 1.16 (s, 2H). ^{13}C NMR; δ 176.30, 165.79, 153.83, 151.85, 148.02, 144.43, 144.36, 138.95, 134.83, 134.00, 131.80, 130.37, 129.16, 128.34, 128.14, 127.05, 124.52, 119.09, 110.85, 107.01, 106.75, 62.93, 49.02, 45.06, 35.82, 30.65, 7.50. MS m/z (%); 521.90 (8.0, M^+). Anal. calcd. For $\text{C}_{27}\text{H}_{24}\text{FN}_3\text{O}_5\text{S}$: C, 62.18; H, 4.64; N, 8.06; S, 6.15. Found: C, 62.04; H, 4.46; N, 8.22; S, 6.52.

4.1.1.5. 7-(4-((2,4-Dimethoxyphenyl)sulfonyl)piperazin-1-yl)-1-ethyl-6-fluoro-4-oxo-1,4-dihydroquinoline-3-carboxylic acid (3a). Yield, 80%; mp 261–262 °C (Hexane/ CH_2Cl_2); IR(KBr) $\nu_{\max}/\text{cm}^{-1}$ 3446 (OH), 1728 (C=O), 1629 (C=O). ^1H NMR (CDCl_3); δ 15.07 (s, br, 1H), 8.69 (s, 1H), 8.15–8.13 (d, 1H, $J = 11.5$ Hz), 7.86–7.85 (d, 1H, $J = 9.0$ Hz), 7.28 (s, 1H), 6.91–6.90 (d, 1H, $J = 6.0$ Hz), 6.56–6.55 (t, 1H, $J = 6.0$ Hz), 4.36–4.28 (t, 2H, $J = 7.0$ Hz), 3.95 (s, 3H), 3.90 (s, 3H), 3.46 (s, 4H), 3.38 (s, 4H), 1.62–1.55 (t, 3H, $J = 6.5$ Hz). ^{13}C NMR; δ 176.99, 167.01, 165.06, 158.59, 154.52, 152.52, 147.28, 145.77, 145.68, 137.06, 133.57, 121.31, 117.85, 113.04, 112.86, 108.55, 104.56, 99.62, 56.09, 55.77, 50.11, 49.79, 45.77, 14.50. MS m/z (%); 519.10 (2.5, M^+). Anal. calcd. For $\text{C}_{24}\text{H}_{26}\text{FN}_3\text{O}_7\text{S}$: C, 55.48; H, 5.04; N, 8.09; S, 6.17. Found: C, 55.90; H, 4.73; N, 8.23; S, 6.09.

4.1.1.6. 1-Cyclopropyl-7-(4-((2,4-dimethoxyphenyl)sulfonyl)piperazin-1-yl)-6-fluoro-4-oxo-1,4-dihydroquinoline-3-carboxylic acid (3b). Yield, 83%; mp 276–277 °C (MeOH/ CH_2Cl_2); IR(KBr) $\nu_{\max}/\text{cm}^{-1}$ 3447 (OH), 1736 (C=O), 1627 (C=O). ^1H NMR (DMSO- d_6); δ 15.15 (s, br, 1H), 8.66 (s, 1H), 7.92–7.89 (d, 1H, $J = 8.0$ Hz), 7.71–7.69 (d, 1H, $J = 9.0$ Hz), 7.59–7.58 (d, 1H, $J = 7.5$ Hz), 6.76 (s, 1H), 6.70–6.68 (dd, 1H, $J = 6.5$, 10.5 Hz), 3.91 (s, 3H), 3.86 (s, 3H), 3.81 (s, 1H), 3.37 (s, 4H), 3.28 (s, 4H), 1.33–1.32 (d, 2H, $J = 6.0$ Hz), 1.17 (s, 2H). ^{13}C NMR; δ 176.33, 165.83, 164.61, 158.41, 148.07, 144.72, 139.04, 132.64, 118.99, 117.07, 111.07, 110.89, 106.97, 106.76, 105.24, 99.550, 79.14, 62.92,

56.13, 55.81, 49.34, 45.32, 35.87, 7.55. MS m/z (%); 531.60 (7.0, M^+). Anal. calcd. For $\text{C}_{25}\text{H}_{26}\text{FN}_3\text{O}_7\text{S}$: C, 56.49; H, 4.93; N, 7.91; S, 6.03. Found: C, 55.27; H, 5.42; N, 8.03; S, 6.14.

4.1.1.7. 7-(4-((3,4-Dimethoxyphenyl)sulfonyl)piperazin-1-yl)-1-ethyl-6-fluoro-4-oxo-1,4-dihydroquinoline-3-carboxylic acid (4a). Yield, 78%; mp 272–273 °C (MeOH/ CH_2Cl_2); IR(KBr) $\nu_{\max}/\text{cm}^{-1}$ 3449 (OH), 1738 (C=O), 1630 (C=O). ^1H NMR (DMSO- d_6); δ 15.24 (s, br, 1H), 8.92 (s, 1H), 7.85–7.83 (d, 1H, $J = 13.0$ Hz), 7.39–7.37 (dd, 1H, $J = 6.5$, 10.0 Hz), 7.22–7.16 (td, 3H, $J = 6.0$, 7.0 Hz), 4.56–4.55 (d, 2H, $J = 6.5$ Hz), 3.86 (s, 6H), 3.40 (s, 4H), 3.10 (s, 4H), 1.39–1.36 (t, 3H, $J = 6.5$ Hz). ^{13}C NMR; δ 176.06, 165.97, 153.69, 152.67, 151.71, 148.74, 148.50, 144.73, 144.65, 136.95, 125.92, 123.85, 121.49, 119.64, 111.43, 110.13, 107.08, 106.49, 62.92, 55.85, 49.02, 48.77, 45.62, 14.29. MS m/z (%); 519.90 (10.0, M^+).

4.1.1.8. 1-Cyclopropyl-7-(4-((3,4-dimethoxyphenyl)sulfonyl)piperazin-1-yl)-6-fluoro-4-oxo-1,4-dihydroquinoline-3-carboxylic acid (4b). Yield, 75%; mp 268–269 °C (MeOH/ CH_2Cl_2); IR(KBr) $\nu_{\max}/\text{cm}^{-1}$ 3447 (OH), 1738 (C=O), 1630 (C=O). ^1H NMR (DMSO- d_6); δ 15.09 (s, br, 1H), 8.63 (s, 1H), 7.85–7.83 (d, 1H, $J = 13.0$ Hz), 7.55–7.54 (d, 1H, $J = 12.0$ Hz), 7.40–7.38 (dd, 1H, $J = 6.5$, 10.0 Hz), 7.22–7.21 (t, 2H, $J = 8.0$ Hz), 3.86 (s, 6H), 3.79 (s, 1H), 3.41 (s, 4H), 3.12 (s, 4H), 1.32–1.31 (d, 2H, $J = 5.0$ Hz), 1.15 (s, 2H). ^{13}C NMR; δ 176.27, 165.77, 152.68, 151.85, 148.76, 147.99, 144.43, 144.35, 138.95, 125.93, 121.50, 119.06, 119.00, 111.45, 111.02, 110.83, 110.13, 106.95, 106.74, 62.93, 55.85, 48.67, 45.58, 35.83, 7.52. MS m/z (%); 531.10 (14.0, M^+).

4.1.1.9. 7-(4-((2,4-Difluorophenyl)sulfonyl)piperazin-1-yl)-1-ethyl-6-fluoro-4-oxo-1,4-dihydroquinoline-3-carboxylic acid (5a). Yield, 90%; mp 199–200 °C (MeOH); IR(KBr) $\nu_{\max}/\text{cm}^{-1}$ 3448 (OH), 1728 (C=O), 1629 (C=O). ^1H NMR (DMSO- d_6); δ 15.14 (s, br, 1H), 8.99 (s, 1H), 7.99 (s, 1H), 7.76–7.74 (d, 2H, $J = 7.5$ Hz), 7.55–7.54 (d, 1H, $J = 8.0$ Hz), 7.14 (s, 1H), 4.44 (s, 2H), 3.40 (s, 4H), 3.29 (s, 4H), 1.41 (s, 3H). MS m/z (%); 495.20 (5.0, M^+).

4.1.1.10. 1-Cyclopropyl-7-(4-((2,4-difluorophenyl)sulfonyl)piperazin-1-yl)-6-fluoro-4-oxo-1,4-dihydroquinoline-3-carboxylic acid (5b). Yield, 86%; mp 186–187 °C (EtOH); IR(KBr) $\nu_{\max}/\text{cm}^{-1}$ 3448 (OH), 1728 (C=O), 1630 (C=O). ^1H NMR (DMSO- d_6); δ 15.11 (s, br, 1H), 8.68 (s, 1H), 8.16 (s, 1H), 7.98–7.96 (d, 1H, $J = 8.5$ Hz), 7.89–7.87 (d, 2H, $J = 13.5$ Hz), 7.76–7.75 (d, 1H, $J = 8.0$ Hz), 3.88–3.87 (d, 1H, $J = 5.5$ Hz), 3.45 (s, 4H), 3.26 (s, 4H), 1.31–1.30 (d, 2H, $J = 6.5$ Hz), 1.17 (s, 2H). MS m/z (%); 507.60 (12.0, M^+).

4.1.1.11. 7-(4-((2,4-Dichlorophenyl)sulfonyl)piperazin-1-yl)-1-ethyl-6-fluoro-4-oxo-1,4-dihydroquinoline-3-carboxylic acid (6a). Yield, 77%; mp 255–256 °C (EtOH); IR(KBr) $\nu_{\max}/\text{cm}^{-1}$ 3448 (OH), 1719 (C=O), 1615 (C=O). ^1H NMR (DMSO- d_6); δ 8.99 (s, 1H), 8.33 (s, 1H), 8.03 (s, 2H), 7.96 (s, 1H), 7.79 (s, 1H), 4.58 (s, 2H), 3.43 (s, 8H, overlapped with DMSO), 1.40 (s, 3H). ^{13}C NMR; δ 176.00, 166.00, 148.50, 144.50, 139.00, 133.00, 132.50, 132.00, 127.50, 114.00, 112.00, 106.50, 79.14, 62.92, 48.00, 45.15, 14.00. MS m/z (%); 527.80 (2.0, M^+). Anal. calcd. For $\text{C}_{22}\text{H}_{20}\text{Cl}_2\text{FN}_3\text{O}_5\text{S}$: C, 50.01; H, 3.82; N, 7.95; S, 6.07. Found: C, 50.86; H, 3.82; N, 7.96; S, 5.25.

4.1.1.12. 1-Cyclopropyl-7-(4-((2,4-dichlorophenyl)sulfonyl)piperazin-1-yl)-6-fluoro-4-oxo-1,4-dihydroquinoline-3-carboxylic acid (6b). Yield, 76%; mp 304–305 °C (AcOH); IR(KBr) $\nu_{\max}/\text{cm}^{-1}$ 3448 (OH), 1719 (C=O), 1630 (C=O). ^1H NMR (DMSO- d_6); δ 15.15 (s, br, 1H), 8.68 (s, 1H), 8.32 (s, 1H), 8.04–8.02 (d, 1H, $J = 8.5$ Hz), 7.95–7.92 (d, 1H, $J = 13.5$ Hz), 7.71–7.69 (dd, 1H, $J = 6.5$, 10.5 Hz), 7.61–7.60 (d, 1H, $J = 6.0$ Hz), 3.76 (s, 1H), 3.44 (s, 4H), 3.40 (s, 4H), 1.33–1.31 (d, 2H, $J = 5.5$ Hz), 1.18 (s, 2H). MS m/z (%); 540.50 (3.0, M^+). Anal. calcd. For

C₂₃H₂₀Cl₂FN₃O₅S: C, 51.12; H, 3.73; N, 7.78; S, 5.93. Found: C, 50.31; H, 3.58; N, 7.93; S, 6.29.

4.1.1.13. 7-(4-((3,4-Dichlorophenyl)sulfonyl)piperazin-1-yl)-1-ethyl-6-fluoro-4-oxo-1,4-dihydroquinoline-3-carboxylic acid (**7a**). Yield, 72%; mp 285–286 °C (AcOH); IR(KBr) $\nu_{\max}/\text{cm}^{-1}$ 3446 (OH), 1729 (C=O), 1630 (C=O). ¹H NMR (DMSO-d₆); δ 15.19 (s, br, 1H), 8.96 (s, 1H), 7.97–7.94 (t, 2H, *J* = 8.0 Hz), 7.79–7.77 (t, 2H, *J* = 7.0 Hz), 7.10–7.08 (d, 1H, *J* = 9.5 Hz), 4.59–4.58 (d, 2H, *J* = 6.5 Hz), 3.43 (s, 4H), 3.20 (s, 4H), 1.40 (s, 3H). ¹³C NMR; δ 166.00, 149.58, 148.65, 137.03, 136.68, 136.09, 135.33, 132.62, 131.91, 129.19, 127.64, 123.87, 111.34, 107.13, 106.69, 62.92, 49.05, 48.82, 45.53, 14.32. MS *m/z* (%); 528.90 (5.5, M⁺).

4.1.1.14. 1-Cyclopropyl-7-(4-((3,4-dichlorophenyl)sulfonyl)piperazin-1-yl)-6-fluoro-4-oxo-1,4-dihydroquinoline-3-carboxylic acid (**7b**). Yield, 70%; mp 316–317 °C (AcOH); IR(KBr) $\nu_{\max}/\text{cm}^{-1}$ 3447 (OH), 1736 (C=O), 1645 (C=O). ¹H NMR (DMSO-d₆); δ 15.14 (s, br, 1H), 8.67 (s, 1H), 8.02 (s, 1H), 7.97–7.96 (d, 1H, *J* = 8.5 Hz), 7.93–7.91 (d, 1H, *J* = 13.0 Hz), 7.79–7.77 (d, 1H, *J* = 8.5 Hz), 7.59–7.58 (d, 1H, *J* = 6.0 Hz), 3.82–3.81 (d, 1H, *J* = 5.0 Hz), 3.43 (s, 4H), 3.22 (s, 4H), 1.33–1.31 (d, 2H, *J* = 6.0 Hz), 1.16 (s, 2H). MS *m/z* (%); 540.20 (17.0, M⁺).

4.2. Synthesis of compounds 8–11

A mixture of arenesulfonyl chloride (1.2 mmol) (Scheme 1), norfloxacin or ciprofloxacin (1 mmol) and K₂CO₃ (152 mg, 1.1 mmol) in dimethylformamide (DMF) (5 ml) was heated at 50 °C for 12 h. The solvent was removed under reduced pressure. Water was added to the residue; the solids were filtered, washed with H₂O and crystallized from the appropriate solvent.

4.2.1. 1-Ethyl-6-fluoro-4-oxo-7-(4-((2,4,6-trichlorophenyl)sulfonyl)piperazin-1-yl)-1,4-dihydroquinoline-3-carboxylic acid (**8a**)

Yield, 68%; mp 323–324 °C (AcOH); IR(KBr) $\nu_{\max}/\text{cm}^{-1}$ 3446 (OH), 1738 (C=O), 1628 (C=O). ¹H NMR (DMSO-d₆); δ 15.23 (s, br, 1H), 8.93 (s, 1H), 7.95–7.92 (d, 1H, *J* = 13.0 Hz), 7.33 (s, 2H), 7.23–7.22 (d, 1H, *J* = 6.0 Hz), 4.14–4.12 (t, 2H, *J* = 6.0 Hz), 3.36 (s, 4H), 3.28 (s, 4H), 1.39–1.38 (d, 3H, *J* = 6.0 Hz). ¹³C NMR; δ 176.06, 166.05, 153.74, 153.42, 151.21, 148.55, 144.75, 137.03, 129.29, 123.99, 120.03, 111.36, 111.18, 106.50, 49.08, 43.61, 28.80, 24.58, 23.33, 14.40. MS *m/z* (%); 562.6 (13.0, M⁺).

4.2.2. 1-Cyclopropyl-6-fluoro-4-oxo-7-(4-((2,4,6-trichlorophenyl)sulfonyl)piperazin-1-yl)-1,4-dihydroquinoline-3-carboxylic acid (**8b**)

Yield, 63%; mp 331–332 °C (AcOH); IR(KBr) $\nu_{\max}/\text{cm}^{-1}$ 3446 (OH), 1740 (C=O), 1628 (C=O). ¹H NMR (DMSO-d₆); δ 15.10 (s, br, 1H), 8.78 (s, 1H), 8.12 (s, 1H), 7.95 (s, 1H), 7.89–7.87 (d, 1H, *J* = 8.5 Hz), 7.23 (s, 1H), 3.87 (s, 1H), 3.37 (s, 4H), 3.29 (s, 4H), 1.33–1.31 (d, 2H, *J* = 5.0 Hz), 1.19 (s, 2H). MS *m/z* (%); 574.2 (4.0, M⁺).

4.2.3. 1-Ethyl-6-fluoro-7-(4-(mesitylsulfonyl)piperazin-1-yl)-4-oxo-1,4-dihydroquinoline-3-carboxylic acid (**9a**)

Yield, 76%; mp 250–251 °C (EtOH); IR(KBr) $\nu_{\max}/\text{cm}^{-1}$ 3449 (OH), 1721 (C=O), 1632 (C=O). ¹H NMR (DMSO-d₆); δ 15.28 (s, br, 1H), 8.96 (s, 1H), 8.32 (s, 2H), 7.94–7.92 (d, 1H, *J* = 13.0 Hz), 7.23–7.22 (d, 1H, *J* = 6.0 Hz), 4.59–4.57 (d, 2H, *J* = 6.0 Hz), 3.35 (s, 4H), 3.26 (s, 4H), 2.60 (s, 6H), 2.30 (s, 3H), 1.41–1.38 (t, 3H, *J* = 6.0 Hz). ¹³C NMR; δ 176.16, 166.00, 153.85, 151.86, 148.59, 145.03, 144.94, 142.77, 139.80, 137.05, 131.92, 130.93, 119.85, 111.29, 111.11, 107.13, 106.68, 79.14, 62.92, 49.03, 43.77, 22.40, 20.43, 14.39. MS *m/z* (%); 501.6 (3.5, M⁺).

4.2.4. 1-Cyclopropyl-6-fluoro-7-(4-(mesitylsulfonyl)piperazin-1-yl)-4-oxo-1,4-dihydroquinoline-3-carboxylic acid (**9b**)

Yield, 78% [39]; mp 238–239 °C (EtOH); IR(KBr) $\nu_{\max}/\text{cm}^{-1}$ 3446 (OH), 1741 (C=O), 1635 (C=O). ¹H NMR (DMSO-d₆); δ 15.15 (s, br, 1H), 8.67 (s, 1H), 8.32 (s, 1H), 7.94–7.92 (d, 1H, *J* = 13.5 Hz), 7.60–7.59 (d, 1H, *J* = 7.0 Hz), 7.13 (s, 1H), 3.80 (s, 1H), 3.37 (s, 4H), 3.28 (s, 4H), 2.60 (s, 6H), 2.30 (s, 3H), 1.32–1.31 (d, 2H, *J* = 5.5 Hz), 1.17 (s, 2H). ¹³C NMR; δ 165.83, 148.07, 142.80, 139.83, 131.95, 130.89, 111.10, 107.06, 106.78, 79.14, 62.93, 48.89, 43.76, 35.89, 22.42, 20.44, 7.55. MS *m/z* (%); 513.6 (11.0, M⁺).

4.2.5. 1-Ethyl-6-fluoro-4-oxo-7-(4-((2,4,6-tri-isopropylphenyl)sulfonyl)piperazin-1-yl)-1,4-dihydroquinoline-3-carboxylic acid (**10a**)

Yield, 64%; mp 301–302 °C (Hexane/CH₂Cl₂); IR(KBr) $\nu_{\max}/\text{cm}^{-1}$ 3447 (OH), 1728 (C=O), 1628 (C=O). ¹H NMR (CDCl₃); δ 15.01 (s, br, 1H), 8.64 (s, 1H), 8.02–7.99 (d, 1H, *J* = 12.5 Hz), 7.21 (s, 2H), 6.87 (s, 1H), 4.21–4.18 (t, 2H, *J* = 6.5 Hz), 3.45 (s, 5H), 3.40 (s, 5H), 2.94–2.92 (t, 1H, *J* = 6.5 Hz), 1.58 (s, 3H), 2.94–2.92 (d, 18H, *J* = 6.0 Hz). ¹³C NMR; δ 176.84, 167.02, 154.44, 153.76, 152.44, 151.88, 147.22, 145.55, 145.47, 137.03, 129.22, 124.11, 121.01, 120.95, 112.93, 112.74, 108.31, 104.43, 49.79, 49.48, 44.03, 34.22, 29.43, 24.92, 23.56, 14.52. MS *m/z* (%); 586.0 (4.0, M⁺). Anal. calcd. For C₃₁H₄₀FN₃O₅S: C, 63.57; H, 6.88; N, 7.17; S, 5.47. Found: C, 63.96; H, 6.64; N, 7.40; S, 5.86.

4.2.6. 1-Cyclopropyl-6-fluoro-4-oxo-7-(4-((2,4,6-tri-isopropylphenyl)sulfonyl)piperazin-1-yl)-1,4-dihydroquinoline-3-carboxylic acid (**10b**)

Yield, 67%; mp 293–294 °C (hexane/CH₂Cl₂); IR(KBr) $\nu_{\max}/\text{cm}^{-1}$ 3447 (OH), 1727 (C=O), 1631 (C=O). ¹H NMR (CDCl₃); δ 14.87 (s, br, 1H), 8.65 (s, 1H), 7.91–7.89 (d, 1H, *J* = 12.5 Hz), 7.37–7.35 (d, 1H, *J* = 6.5 Hz), 7.21 (s, 2H), 4.20–4.18 (t, 2H, *J* = 6.5 Hz), 3.44 (s, 5H), 3.41 (s, 4H), 2.94–2.92 (t, 1H, *J* = 6.5 Hz), 1.40–1.39 (d, 2H, *J* = 5.0 Hz), 1.30–1.28 (d, 18H, *J* = 6.5 Hz), 1.20 (s, 2H). ¹³C NMR; δ 176.87, 166.73, 154.56, 153.74, 152.56, 151.87, 147.44, 145.30, 145.22, 138.96, 129.24, 124.11, 120.12, 120.06, 112.43, 112.24, 107.93, 105.36, 49.35, 49.33, 44.03, 35.40, 34.21, 29.42, 24.92, 23.56, 9.24. MS *m/z* (%); 597.7 (7.0, M⁺). Anal. calcd. For C₃₂H₄₀FN₃O₅S: C, 64.30; H, 6.75; N, 7.03; S, 5.36. Found: C, 64.70; H, 6.56; N, 7.15; S, 5.44.

4.2.7. 1-Ethyl-6-fluoro-4-oxo-7-(4-((2,3,4,5,6-pentamethylphenyl)sulfonyl)piperazin-1-yl)-1,4-dihydroquinoline-3-carboxylic acid (**11a**)

Yield, 59%; mp 309–310 °C (MeOH); IR(KBr) $\nu_{\max}/\text{cm}^{-1}$ 3446 (OH), 1728 (C=O), 1629 (C=O). ¹H NMR (DMSO-d₆); δ 15.30 (s, br, 1H), 8.97 (s, 1H), 7.95 (s, 1H), 7.36 (s, 1H), 4.60 (s, 2H), 3.33 (s, 4H, overlapped with DMSO), 3.27 (s, 4H), 2.55 (s, 6H), 2.28 (s, 3H), 2.24 (s, 6H), 1.40 (s, 3H). MS *m/z* (%); 529.2 (10.0, M⁺). Anal. calcd. For C₂₇H₃₂FN₃O₅S: C, 61.23; H, 6.09; N, 7.93; S, 6.05. Found: C, 61.59; H, 6.31; N, 8.13; S, 6.33.

4.2.8. 1-Cyclopropyl-6-fluoro-4-oxo-7-(4-((2,3,4,5,6-pentamethylphenyl)sulfonyl)piperazin-1-yl)-1,4-dihydroquinoline-3-carboxylic acid (**11b**)

Yield, 58%; mp 316–317 °C (Hexane/CH₂Cl₂); IR(KBr) $\nu_{\max}/\text{cm}^{-1}$ 3447 (OH), 1727 (C=O), 1630 (C=O). ¹H NMR (CDCl₃); δ 14.88 (s, br, 1H, exchange with D₂O), 8.70 (s, 1H), 7.96–7.93 (d, 1H, *J* = 8.0 Hz), 7.36–7.35 (d, 1H, *J* = 6.5 Hz), 3.55 (s, 1H), 3.44 (s, 4H), 3.38 (s, 4H), 2.60 (s, 6H), 2.32 (s, 3H), 2.27 (s, 6H), 1.40–1.39 (d, 4H, *J* = 5.5 Hz). ¹³C NMR; δ 176.97, 166.71, 147.47, 145.30, 140.64, 138.96, 136.02, 135.08, 132.81, 112.39, 108.16, 105.31, 49.37, 44.05, 35.31, 18.86, 17.92, 17.85, 17.08, 8.23. MS *m/z* (%); 541.9 (4.6, M⁺). Anal. calcd. For C₂₈H₃₂FN₃O₅S: C, 62.09; H, 5.95; N, 7.76; S, 5.92. Found: C, 62.31; H, 5.93; N, 7.91; S, 5.92.

4.3. Antibacterial methodology

MIC of the arenesulfonyl derivatives **1–11** and the reference drug ciprofloxacin were performed by broth dilution method as proposed by Clinical and Laboratory Standards Institute [35] and interpreted using its guidelines. Briefly, the compounds were dissolved in dimethylsulphoxide to give final concentration 5120 µg/mL, and then tenfold dilution was made in the Mueller–Hinton broth (MHB), which was supplied from Oxoid Chemical Co. UK., to give final concentration 512 µg/mL. Mueller-Hinton broth 100 µL was dispensed into wells of sterile 96 microtitre plate. A 100 µL of the tested compounds (512 µg/mL) was pipetted into the wells in first column and mixed the contents by using multipipettor by sucking up and down 6–8 times. Then 100 µL from the first column was withdrawn and added to the second column to make a twofold dilution. This procedure was repeated down to 12th column to reach the concentration of 0.25 µg/mL. A 100 µL was discarded from 12th column. The standard strains, *S. aureus* ATCC 29213, *Bacillus subtilis* ATCC 10400, *E. coli* ATCC 25922 and *P. aeruginosa* ATCC 27853 were grown in the tryptone soy broth to the right A600. Five µL of bacterial inoculums (10^4 – 10^5 CFU/mL) was dispensed into wells. The plates were incubated at 35 °C for 18 h. After the incubation period, the results of MIC were recorded manually and interpreted according to the recommendations of Laboratory Standards Institute [35]. MIC is defined as the lowest concentration of the drug that kills or inhibits visible growth of microorganism.

4.4. Molecular modeling methods

4.4.1. Energy minimization and alignment of molecules

All 23 compounds were built on workspace of molecular modeling software VLife MDS 3.5 [36]. The structures were then converted to three-dimensional space for further analysis. All molecules were batch optimized for the minimization of energies using Merck molecular force field (MMFF) [41] followed by considering distance-dependent dielectric constant of 1.0, convergence criterion or root mean-square (RMS) gradient at 0.01 kcal/molÅ and the iteration limit to 10,000. The energy-minimized geometry was used for the calculation of fieldalign and the various 2D descriptors. All molecules were aligned by an atom based alignment technique using a common structure as a template. The most active compound **3b** was used as the template for alignment of molecule. The alignment is useful for studying shape variation with respect to the base structure selected for alignment.

4.4.2. 2D-descriptor calculations

4.4.2.1. Data set. A data set of 22 compounds of arenesulfonyl derivatives along with reference ciprofloxacin was used for the present 2D-QSAR study. There is high structural diversity and a sufficient range of the biological activity in the selected series of these derivatives. The biological activity values [MIC (µmol/mL)] were converted to negative logarithmic scale ($-\log 1/\text{MIC}$) and subsequently used as the dependent variable for the QSAR analysis. The energy-minimized geometry of the compounds was used for the calculation of the various 2D descriptors (Individual, Chi, ChiV, Path count, ChiChain, ChiVChain, Chainpathcount, Cluster, Pathcluster, Kapa, Element Count, Estate number, Estate contribution, Semi-empirical, Hydrophilic–hydrophobic and Polar surface area). The various Alignment Independent (AI) descriptors were also calculated. For calculation of alignment, the independent descriptor was assigned the utmost three attributes. The first attribute was T to characterize the topology of the molecule. The second attribute was the atom type, and the third attribute was assigned to atoms taking part in the double or triple bond. The pre-processing of the

independent variables (i.e., 2D descriptors) was done by removing invariable (constant column).

4.4.2.2. Statistical analysis. The descriptors were taken as independent variables and biological activity as dependent variable. Multiple Linear Regression (MLR) method of analysis was used to derive the 2D-QSAR equations. The developed QSAR models are evaluated using the following statistical measures: r^2 , (the squared correlation coefficient); r^2_{se} , (standard error of squared correlation coefficient); F test, (Fischer's value) for statistical significance; q^2 , (cross-validated correlation coefficient); q^2_{se} , (standard error of cross-validated square correlation coefficient); pred_r^2 , (r^2 for external test set); $\text{pred}_r^2_{\text{se}}$, (standard error of predicted squared regression); Z -score, (Z -score calculated by the randomization test); $\text{best_ran_}q^2$, (highest q^2 value in the randomization test). The regression coefficient r^2 is a relative measure of fit by the regression equation. It represents the part of the variation in the observed data that is explained by the regression. However, a QSAR model is considered to be predictive, if the following conditions are satisfied: $r^2 > 0.6$, $q^2 > 0.6$ and $\text{pred}_r^2 > 0.5$ [42]. The F -test reflects the ratio of the variance explained by the model and the variance due to the error in the regression. High values of the F -test indicate that the model is statistically significant. The low standard error of r^2 (r^2_{se}), q^2 (q^2_{se}) and pred_r^2 ($\text{Pred}_r^2_{\text{se}}$) shows absolute quality of fitness of the model.

4.4.3. Docking methodology

Docking studies have been performed using MOE 2008.10. With this purpose, crystal structure of topoisomerase II DNA gyrase, with its bound inhibitor ciprofloxacin (PDB codes: 2XCT) was obtained from the Protein Data Bank in order to prepare protein for docking studies. Docking procedure was followed using the standard protocol implemented in MOE 2008.10 and the geometry of resulting complexes was studied using the MOE's Pose Viewer utility.

Acknowledgments

The authors extend their appreciation to the Deanship of Scientific Research at King Saud University for funding the work through the research group project no. RGP-VPP-163. Our sincere acknowledgments to Chemical Computing Group Inc, 1010 Sherbrooke Street West, Suite 910, Montreal, H3A 2R7, Canada, for its valuable agreement to use the package of MOE 2008.10 software.

References

- [1] H. Koga, A. Itoh, S. Murayama, S. Suzue, T. Irikura, J. Med. Chem. 23 (1980) 1358.
- [2] Y. Goueffon, G. Montay, F. Roquet, M.C.R. Pesson, Acad. Sci. 292 (1971) 37.
- [3] K. Sata, Y. Matsuura, M. Inoue, T. Une, Y. Osada, H. Ogawa, S. Mitsuhashi, Antimicrob. Agents Chemother. 22 (1982) 548.
- [4] R. Wise, J.M. Andrews, L.J. Edwards, Antimicrob. Agents Chemother. 23 (1983) 559.
- [5] J.M. Domagala, C.L. Heifetz, M.P. Hutt, T.F. Mich, J.B. Nichols, M. Solomon, D.F. Worth, J. Med. Chem. 31 (1988) 991–1001.
- [6] D.C. Hooper, J.S. Wolfson, in: Quinolone Antimicrobial Agents, second ed. (1993).
- [7] D.C. Hooper, Clin. Infect. Dis. 32 (Suppl. 1) (2001) S9.
- [8] M.T. Mascellino, S. Farinelli, F. Iegri, E. Inoa, C. De Simone, Drug Exp. Clin. Res. 24 (1998) 139.
- [9] W.A. Petri Jr, in: J.G. Hardman, L.E. Limbird, A.G. Gilman (Eds.), Goodman and Gilman's The Pharmacological Basis of Therapeutics, 10th ed. McGraw-Hill, New York, 2001, pp. 1179–1183.
- [10] V.T. Andriol, Drugs 2 (1999) 1.
- [11] J.M. Domagala, L.D. Hanna, C.L. Heifetz, M.P. Hutt, T.F. Mich, J.P. Sanchez, M. Solomon, J. Med. Chem. 29 (1986) 394.
- [12] L.L. Shen, L.A. Mitscher, P.N. Sharma, T.J. O'Donnell, D.W.T. Chu, C.S. Cooper, T. Rosen, A.G. Pernet, Biochemistry 28 (1989) 3886.
- [13] A. Foroumadi, S. Emami, A. Davood, M.H. Moshafi, A. Sharifian, M. Tabatabaie, H. Tarhimi Farimani, G. Sepehri, A. Shafiee, Pharm. Sci. 3 (1997) 559.

- [14] M. Mirzaie, A. Foroumadi, *Pharm. Pharm. Commun.* 6 (2000) 351.
- [15] K.C. Fang, Y.L. Chen, J.Y. Sheu, T.C. Wang, C.C. Tzeng, *J. Med. Chem.* 43 (2000) 3809.
- [16] Y.L. Chen, K.C. Fang, J.Y. Sheu, S.L. Hsu, C.C. Tzeng, *J. Med. Chem.* 44 (2001) 2374.
- [17] A. De Sarro, G. De Sarro, *Curr. Med. Chem.* 8 (2001) 371.
- [18] V.E. Anderson, N. Osheroff, *Curr. Pharm. Des.* 7 (2001) 339.
- [19] D.C. Hooper, E. Rubinstein, in: *Quinolone Antimicrobial Agents*, ASM Press American Society for Microbiology, Washington, USA, 2003.
- [20] J.M. Blondeau, *Survey Ophthalmol.* 49 (Suppl. 2) (2004) S73.
- [21] R.H. Manzo, D.A. Allemanni, J.D. Perez, U.S. Patent 5,395,936 (1995).
- [22] D. Allemanni, F. Alovero, R. Manzo, *J. Antimicrob. Chemother.* 34 (1994) 261.
- [23] F. Alovero, M. Nieto, M. Mazzieri, R. Then, R. Manzo, *Antimicrob. Agents Chemother.* 42 (6) (1998) 1495.
- [24] M. Nieto, F. Alovero, R. Manzo, M. Mazzieri, *Eur. J. Med. Chem.* 34 (1999) 209.
- [25] F. Alovero, A. Barnes, M. Nieto, M. Mazzieri, R. Manzo, *J. Antimicrob. Chemother.* 48 (5) (2001) 709.
- [26] F. Alovero, X.-S. Pan, J. Morris, R. Manzo, L. Fisher, *Antimicrob. Agents Chemother.* 44 (2) (2000) 320.
- [27] X.-S. Pan, P. Hamlyn, R. Talens-Visconti, F. Alovero, R. Manzo, L. Fisher, *Antimicrob. Agents Chemother.* 46 (8) (2002) 2498.
- [28] J. Heddle, A. Maxwell, *Antimicrob. Agents Chemother.* 46 (2002) 1805.
- [29] M.I. El-Gamal, S.M. Bayomi, S.M. El-Ashry, S.A. Said, A.A.-M. Abdel-Aziz, N.I. Abdel-Aziz, *Eur. J. Med. Chem.* 45 (2010) 1403.
- [30] A.A.-M. Abdel-Aziz, K.E.H. ElTahir, Y.A. Asiri, *Eur. J. Med. Chem.* 46 (2011) 1648.
- [31] M.A. El-Sayed, N.I. Abdel-Aziz, A.A.-M. Abdel-Aziz, A.S. El-Azab, Y.A. Asiri, K.E.H. ElTahir, *Bioorg. Med. Chem.* 19 (2011) 3416.
- [32] A.S. El-Azab, M.A. Al-Omar, A.A.-M. Abdel-Aziz, N.I. Abdel-Aziz, M.A.-A. El-Sayed, A.M. Aleisa, M.M. Sayed-Ahmed, S.G. Abdel-Hamide, *Eur. J. Med. Chem.* 45 (2010) 4188.
- [33] F.A. Al-Omary, L.A. Abou-Zeid, M.N. Nagi, S.E. Habib, A.A.-M. Abdel-Aziz, A.S. El-Azab, S.G. Abdel-Hamide, M.A. Al-Omar, A.M. Al-Obaid, H.I. El-Subbagh, *Bioorg. Med. Chem.* 18 (2010) 2849.
- [34] MOE 2008.10, Chemical Computing Group, Inc.
- [35] Clinical and Laboratory Standards Institute (CLSI), Performance standards for antimicrobial susceptibility tests, Wayne, Pa. European Committee for Antimicrobial Susceptibility Testing (EUCAST) (2003) determination of minimum inhibitory concentrations (MICs) of antibacterial agents by broth dilution. EUCAST discussion document E. Dis 5.1, *Clin. Microbiol. Infect.* 9 (2008) 1–7.
- [36] V-Life Molecular Design Suite 3.5, VLife Sciences Technologies Pvt. Ltd., Available from: www.Vlifesciences.com.
- [37] Fieldalign 2.1 Cresset-BMD, Available from: <http://www.cresset-bmd.com/product/fieldalign>.
- [38] B.D. Bax, P.F. Chan, D.S. Eggleston, A. Fosberry, D.R. Gentry, F. Gorrec, I. Giordano, M.M. Hann1, A. Hennessy, M. Hibbs, J. Huang, E. Jones, J. Jones, K.K. Brown, C.J. Lewis, E.W. May, M.R. Saunders, O. Singh, C.E. Spitzfaden, C. Shen, A. Shillings, A.J. Theobald, A. Wohlkonig, N.D. Pearson, M.N. Gwynn, *Nature* 466 (2010) 935.
- [39] M.J. Nieto, F.L. Alovero, R.H. Manzo, Maria R. Mazzieri, *Eur. J. Med. Chem.* 40 (2005) 361.
- [40] A.-R. Shoaâ, International patent, WO 01/36408 A1, 2001.
- [41] T.A. Halgren, *J. Comput. Chem.* 17 (1996) 490.
- [42] A. Golbraikh, A. Tropsha, *J. Mol. Graph. Model* 20 (2002) 269.